Journal of Natural Sciences Research www.iiste.org
ISSN 2224-3186 (Paper) ISSN 2225-0921 (Online)
Vol.4, No.23, 2014

Integrated Resistivity Sounding and Anisotropy to Hydrogeologic Investigation of Alakuta-Apete Area of Ibadan Southwestern Nigeria

Oladunjoye Micheal Akanji Adesoji Akingbesote Oluwatosin
Department of Geology, University of Ibadan, Ibadan, Nigeria

Abstract
Fast growing population of Alakuta - Apete area of Ibadan has warranted the need to develop the water availability in the area. The area lies within the basement complex terrain of southwestern Nigeria typified by banded gneiss and minor intrusion of pegmatite and quartz vein. This study was carried out to characterize the aquifer units and anisotropic properties of fractures for evaluation of groundwater development in the area. Hydrogeologic investigation was carried out on forty-five wells to study the groundwater system and dynamics in shallow aquifers. This study was integrated with twenty-two Schlumberger vertical electrical soundings to further investigate the different subsurface geomaterials with the aim of delineating the thickness and continuity of the aquiferous zone. Six radial soundings were conducted to study the directional properties of the anisotropic rock and thus indicate the orientation fractures and extent of the fracturing. Measured Static water level and head measured vary from 0.8 to 9.9m and 182m to 209m respectively indicating that groundwater generally flow towards the eastern and southwestern part from two main discharge sites in the northwestern part of the study area. Interpretation of the twenty-two Schlumberger vertical electrical soundings generally shows three layered earth structure notably top soil, saturated/sandy/lateritic clay and weathered/fractured/fresh basement which are mostly of the "H" curve type. Overburden isopach map revealed that the depth to the bedrock varies from 3m to 23m. The main aquifer (weathered basement) is relatively shallow and most wells in the study area terminate in the second layer. The main water – bearing unit in the area of study is the weathered basement and the fractured basement which are within the second and third geoelectric layers respectively. The weathered/fractured basement resistivity values vary from 62 Ohm-m and 9807 Ohm-m with thickness values ranging from 2.2m to 36m. Polygons produced from six radial sounding showed the predominant structural trends of fractures on the banded gneiss. The radial resistivity survey results show that there is significant anisotropy between 0 – 50 m depth generally striking NE-SW, NW-SE and N-S showing the major structural trend of basement fractures. Coefficient of Resistivity Anisotropy ranges between 1.03 and 1.38. Variation of apparent resistivity is strongest at the eastern and southern parts of the study area with coefficients of 1.33, 1.38, and 1.30. This high coefficient of anisotropy implies higher- permeability anisotropy. The directionality of the trends could be responsible for the depressions in the weathered/fractured basement. The regions with thick weathered/fractured basement/depressed zones are likely to be most promising sites for borehole drilling.
Keywords: coefficient of resistivity anisotropy

I. INTRODUCTION

Groundwater exploration in crystalline basement complex terrain requires detailed geophysical data investigation to effectively characterize the hydrogeologic zones and to enhance successful identification of well locations. These zones are largely due to the development of secondary porosity and permeability by fracturing and/or weathering of these rocks. Thus, the search for groundwater in such rocks is aimed at mapping such secondary structures which constitute the basement aquifers.

Alakuta is undoubtedly undergoing rapid development due to increased population and expansion of residential sites in Apete, Ibadan. This has demanded for improved basic amenities especially portable water supply for domestic use. Existing hand dug wells in the area are only productive in the raining season but are at least low yielding during the dry season. Recent growth in student and staff populations has imposed significant stress on the existing inadequate water scheme, based solely on groundwater abstraction from boreholes around the campus. Consequently, it became very expedient to expand the existing water scheme. The focus was to delineate the area into hydrogeologic zones in order to increase the number of effective boreholes in the area

Several researchers have worked on the groundwater development of southwestern Nigeria. Olorunfemi (1990), Olayinka and Olorunfemi (1992), and Olorunfemi et al. (1999.) concluded that occurrence of groundwater in southwestern Nigeria is primarily related to geology and its availability underscored by deep weathering and fracturing. From their studies, it was commonly observed that the unit with low resistivity value representing clayey sand and weathered bedrock, which may be fractured, constituted the main aquifer materials in the area. Also, regolith and fractured bedrock generally occurred in a typical basement terrain (Odusanya and Amadi, 1990). Azimuthal Resistivity Sounding (ARS) has been adopted as a fast and effective surface method for determining the principal directions of the electrical anisotropy that are directly related to structural or lateral lithological changes in the subsurface (Leonard-Mayer 1984; Taylor And Fleming, 1988, Skjernaa And Jørgensen, 1993; Hagrey, 1994; Cohn And Rudman, 1995; Lane et al., 1995, Busby, 2000; Busby And Jackson, 2006). Odoh and Onwuemesi 2009 estimated the anisotropy properties of fractures in Presco Compus of Ebonyi State University Abakaliki Nigeria using Azimuth resistivity survey method. This research was carried out to improve groundwater availability so as to balance the increased population and thus with the objective of evaluating the groundwater potential of the area by mapping the subsurface aquifers, delineating region that are likely to be high yielding and best region for borehole drilling. Integrated Vertical Electrical and Radial Soundings with well data analysis were adopted to achieve the said objective.

Site Description and Geological Setting

The study area, Alakuta-Awotan, is located between latitudes 7^0 26' 10' and 7^0 26' 30''N and longitudes 3^0 51' 20'' and 3^0 51'50"E in Ido-local government area of Ibadan (Fig. 1) covering area extent of about 835m by 1025m. It can be accessed through a major road from Sango to Apete residential areas and drained by Eleyele river and its tributaries. The river occupies the southwestern and southeastern parts of the study area. Geology of Ibadan and environs, including Alakuta area, falls within the Pre-Cambrian rocks of Southwestern Nigeria. The major rock types are schist-quartzites, granite-gneiss, banded gneiss, augen-gneiss, and migmatites (Jones and Hockey, 1964), while minor rock types such as pegmatite, aplites, quartz veins, and dolerite dykes intruded the main rocks in places (Figure 2). Gneisses are migmatized in places, and characterized by predominantly medium-sized grains while schist-quartzites occur as elongated ridges striking NW-SE (Olayinka et al., 1999). The study area area is typified by banded and migmatite gneises which generally stike NW-SE and dip to the east (Fig 2). The joints on the outcrops in the area are mostly oriented perpendicular to the strike (NW-SE) of the rock foliation. Notable N-S and NW-SE plunging minor folds were mapped on the gneiss complex.

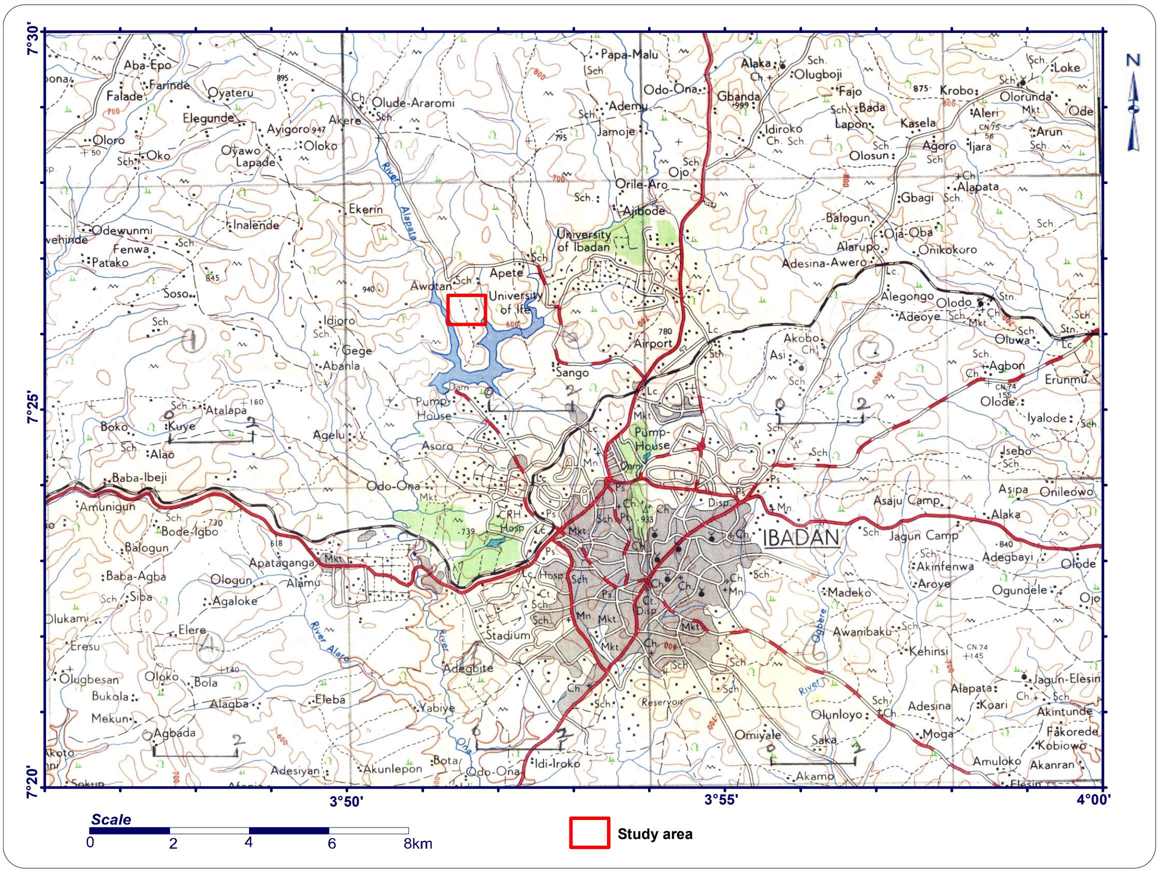

Figure 1. Topographical map of Ibadan showing the study area.

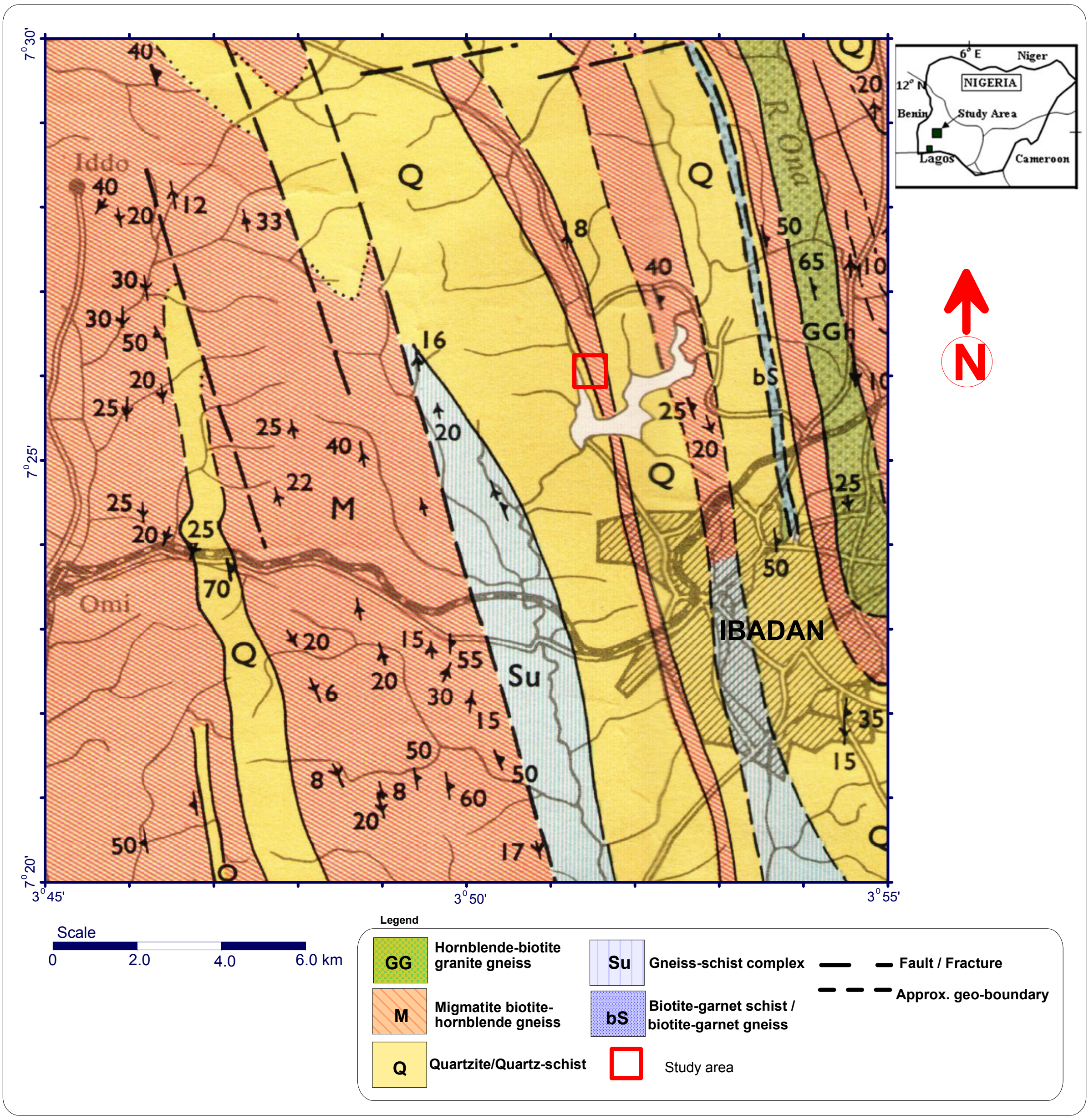

Figure 2: Geological Map of Ibadan showing the study area.

Materials and Methods

Depths to water level, total depth and in some cases depth to visible basement (weathered or fresh) were measured in forty-five wells to give information on the groundwater flow dynamics of the study area. Well positions and their respective elevation relative to the main sea level were determined using Garmin Global Positioning System (GPS). These helped in determining the hydraulic water head in wells and thus groundwater head elevation contour which gave information on the groundwater flow direction. Figure 3 shows the location of the wells in the study area.

Electrical resistivity of the subsurface involved determination of the distribution of ground resistivity based on its response to the flow of electric current injected during surface measurement. True resistivity of subsurface layer are calculated by measuring the potential difference generated to Schlumberger electrode configuration from the apparent resistivity Ra which is given by Ra = DV/I. K, where K is the geometric factor.

Rocks have varying physical properties giving various anisotropies (electrical, magnetic, gravity etc) depending on the rock type, structure, mineral assemblages, fluid content, porosity etc. Electrical resistivity of rock varies in space giving the rock its characteristic electrical anisotropy. A rock is said to be electrically anisotropic if the value of a vector measurement of its resistivity varies with direction (Taylor and Flemming, 1988; Watson and Barke, 1999). This anisotropy may result from rock fracturing, joints and fault systems, rock boundary cracks and aligned mineral grain orientations which are common features of the rocks in the study area. Thus the rocks in the area are expected to exhibit some degrees of electrical anisotropy.

Twenty-two Vertical Electrical Sounding were carried out to generate geoelectric parameters of the different subsurface layers which helped to delineate the aquiferous zones in the subsurface. Selection of the sounding locations was guided by well locations and this also serves as controls for the interpretation of the geophysical data and to proffer reasons for some seasonal wells (Fig. 3). These sounding were conducted using Schlumberger configuration with current electrode spreading ranging from 1m to 100m. The field data were plotted on bi-log paper and partial curve matched using standard two layered master curve (Koefeod, 1979), to obtain some geoelectrical parameters such as layer thickness and layer resistivity and this was latter iterated using RESIST software inversion model.

Six azimuthal resistivity surveys (ARS) were conducted to locate, characterize, and identify the directional properties of anisotropic rock mass in the study area. Their respective locations are shown in Figure 3. The electrode positions were rotated in increments of 45 degree about a central fixed point. The apparent resistivity (measured in Ohm-m) was recorded for all electrodes spacing and plotted along the azimuth on a polar diagram so as to observe the correlation between the measured structural direction and the plotted anisotropy polygon direction. In this azimuthal resistivity survey, any observed change in apparent resistivity ρ_a was interpreted as an indication of fracture anisotropy and thus the orientations of the subsurface fractures. Fracture strikes were identified as the direction of maximum apparent resistivities on the polar plots.

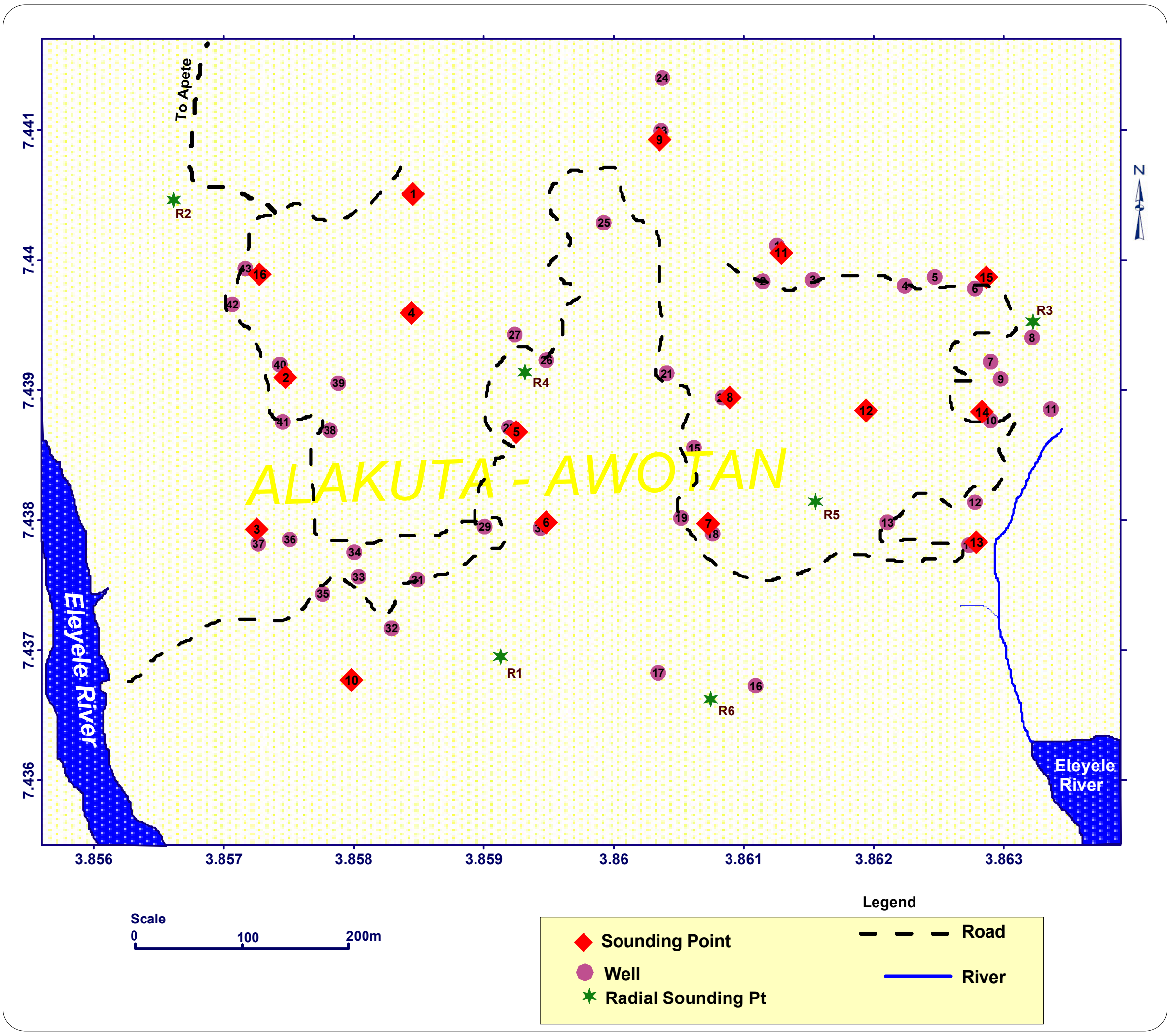

Figure 3. Showing location of wells, vertical electrical and radial sounding points in the study area.

In any formation whose anisotropy is due to the presence of fractures, the apparent resistivity (rf) measured normal to its strike direction is greater than apparent resistivity (rs) measured along the strike direction, when Schlumberger or Werner array is used but contrary when crossed square array method is employed (Lane et al 1995). Coefficient of anisotropy is calculated by $\gamma = \sqrt{(\frac{rt}{rs})}$.

Homogenuity of the subsurface fas been related to the shape of the polygon, an isotropic homogeneous formation assumes a circular polygon shape indicative of anisotropic nature of the formation. The direction of the polygon corresponds to the stike direction of the fracture and ratio of the long to short axis is an indication of the presence of fractures in the area if high, and otherwise if low (Skjernaa and Jorgensen, 1993).

RESULTS AND DISCUSSION

Hydrogeological Investigation Results

Depth to the static water level within the area varies from 0.8m to 9.9m, whereas the water head ranges from 184m (in the northwestern) to 208m (in the southeastern) above sea level (Table 1). Figure 4 is the water head contour map of the study area which shows various directions of groundwater flow. Higher elevation at the northwestern part of the study area indicates that groundwater generally flows toward the eastern and southwestern parts. However two discharge sites (D1and D2) and one recharge site (R1) were established in the flow map existing at the western and eastern parts respectively.

Vertical Electrical Sounding Result

Result of interpretation and plotting of field data generally indicates three to four layered earth structure as summarized in Table 2. Figure 5 shows representative resistivity curves type for H, K and HA for VES 11, 12 and 10. In accordance with available geological information and the multi-layer models obtained from inversion of VES data, geoelectrical cross sections were constructed across four profiles (Fig) 6a, 6b, 6c and 6d. The cross-section revealed a general three to four layered subsurface medium.

The first, uppermost, geoelectrical layer is relatively thin (0.5–2.9 m) and exhibits a wide range of resistivity values (59–1160 Ohm-m) reflecting the effect of surface conditions.

The second layer was recognized as being continuous beneath all stations along most profiles. It exhibits moderate to low resistivity values ranging from 13 to 425 Ohm-m with thickness values ranging from 1.0 to 26.3 m. This layer is composed mainly of weathered layer however; low resistivity in this layer may be due to the presence of clay. Most wells in the study area terminates in this layer thus are capable of producing water for domestic usage.

The third layer represents the main hydrogeologic target for borehole siting with resistivity values (172–9807 Ohm-m). This layer was inferred to be fractured and fresh basement.

From the geoelectric section and wells position along the profile, it can be concluded that most wells terminate in the second layer or on top of the third layer. However well 28 on geoelectric section (figure 6a) was cited on migmatite gneiss outcrop which was severally blasted until adequate potable groundwater was intersected this thus indicates that the rock is sufficiently fractured.

TABLE 1 : WELL DATA, OUTCROP AND RIVER OBSERVED IN THE STUDY AREA

WELL NUMBER	LATITUDE	LONGITUDE	ELEVATION (m)	WATER TABLE(m)	TOTAL DEPTH OF WELL(m)
1	$7^{0}\ 26^{I}\ 22.8^{II}$	$3^{0}\ 51^{I}\ 40.6^{II}$	206	5.71	6.77
2	$7^{0}\ 26^{I}\ 21.8^{II}$	$3^{0}\ 51^{I}\ 40.1^{II}$	201	6.1	NIL
3	$7^{0}\ 26^{I}\ 21.9^{II}$	$3^{0}\ 51^{I}\ 41.4^{II}$	199	5.55	11.7
4	$7^{0}\ 26^{I}\ 21.7^{II}$	$3^{0}\ 51^{I}\ 43.9^{II}$	195	4.8	9
5	$7^{0}\ 26^{I}\ 22.0^{II}$	$3^{0}\ 51^{I}\ 44.8^{II}$	193	4.17	5.8
6	$7^{0}\ 26^{I}\ 22.5^{II}$	$3^{0}\ 51^{I}\ 45.9^{II}$	192	2.8	5.53
7	$7^{0}\ 26^{I}\ 21.9^{II}$	$3^{0}\ 51^{I}\ 46.4^{II}$	191	3.25	4.17
8	$7^{0}\ 26^{I}\ 19.9^{II}$	$3^{0}\ 51^{I}\ 47.4^{II}$	190	3.25	5.42
9	$7^{0}\ 26^{I}\ 18.4^{II}$	$3^{0}\ 51^{I}\ 46.6^{II}$	191	3.2	5.02
10	$7^{0}\ 26^{I}\ 16.9^{II}$	$3^{0}\ 51^{I}\ 46.7^{II}$	189	4.11	5.01
11	$7^{0}\ 26^{I}\ 17.3^{II}$	$3^{0}\ 51^{I}\ 48.0^{II}$	186	2.32	3.12
12	$7^{0}\ 26^{I}\ 14.1^{II}$	$3^{0}\ 51^{I}\ 45.9^{II}$	188	3.07	4.4
13	$7^{0}\ 26^{I}\ 13.5^{II}$	$3^{0}\ 51^{I}\ 43.5^{II}$	189	DRY WELL	9
14	$7^{0}\ 26^{I}\ 12.6^{II}$	$3^{0}\ 51^{I}\ 45.8^{II}$	188	4.2	5.22
15	$7^{0}\ 26^{I}\ 12.1^{II}$	$3^{0}\ 51^{I}\ 44.7^{II}$	190	DRY WELL	3.44
16	$7^{0}\ 26^{I}\ 07.8^{II}$	$3^{0}\ 51^{I}\ 39.8^{II}$	197	4.53	5.96
17	$7^{0}\ 26^{I}\ 08.1^{II}$	$3^{0}\ 51^{I}\ 37.1^{II}$	198	1.6	5.2
18	$7^{0}\ 26^{I}\ 13.3^{II}$	$3^{0}\ 51^{I}\ 38.5^{II}$	201	5.3	6.2

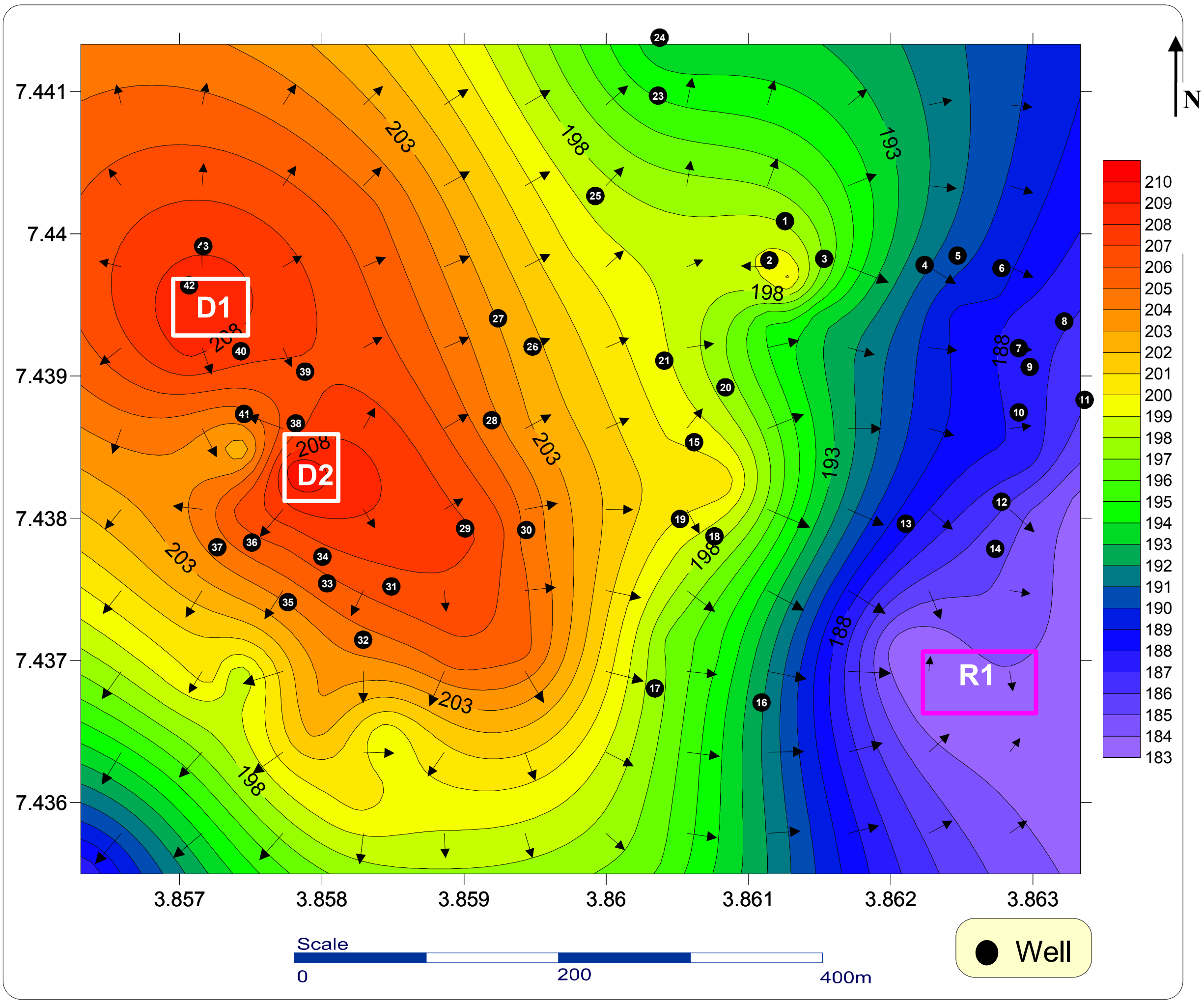

Figure 4. Static water head relief of the study area (D1 and D2 are Discharge areas whereas R1 is Recharge area)

Table 2: Summary of VES interpretation and well data from Alakuta- Awotan

VES NO	RESISTIVITY (Ωm)	THICKNESS (m)	DEPTH (m)	PROBABLE LITHOLOGY	CURVE TYPE
1	173	1.1	1.1	Top soil	H
	55	6.5	7.6	Weathered Basement(Clayey)	
	570	-		Fractured Basement	
2	296	0.9	0.9	Top soil	H
	74	3.7	4.6	Weathered Basement(Clayey)	
	1308	-	-	Fresh Basement	
3	166	1.2	1.2	Top soil	H
	26	1.0	2.2	Weathered Basement (saturated Clay)	
	863	-		Fresh Basement	
4	115	0.5	0.5	Top soil	A
	219	10.8	11.3	Lateritic clay	
	312	-	-	Weathered Basement	
5	1160	0.2	0.2	Top soil	H
	78	3.3	3.5	Weathered Basement (Clayey)	
	491	-	-	Fractured Basement	
6	143	0.8	0.8	Top soil	
	425	1.6	2.4	Compacted lateritic clay	
	160	3.8	6.2	Weathered basement (clayey sand)	
	393	-	-	Fractured Basement	
7	207	0.7	0.7	Top soil	KH
	399	4.7	5.4	Compacted lateritic clay	
	45	17.2	22.6	Weathered Basement (Saturated Clay)	
	446			Fractured Basement	
8	78	1.2	1.2	Top soil	K
	154	6.6	7.9	Clayey sand	
	62	-	-	Highly weathered basement	
9	304	0.9	0.9	Top soil	H
	114	22.6	23.5	Weathered Basement (clayey sand)	
	272	-	-	Fractured Basement	
10	252	0.6	0.6	Top soil	
	95	3.1	3.7	Clayey soil	
	175	13.7	17.4	Weathered Basement (clayey sand)	
	9807	-		Fresh Basement	
11	59	2.1	2.1	Top soil	K
	224	6.6	8.7	Lateritic clay	
	140	-	-	Weathered Basement (clayey sand)	
12	132	0.5	0.5	Top soil	H
	81	23.6	24.1	Sandy clay	
	18	-	-	Highly Weathered Basement	
13	107	0.7		Top soil	
	79	13.8	14.5	Weathered basement (clayey)	
	365 -	-	-	Fractured Basement	
14	211	0.9	0.9	Top soil	H
	45	3.9	4.7	Weathered Basement(Saturated Clay)	
	137	-	-	Fractured Basement	
15	98	2.3	2.3	Top soil	H
	18	2.5	4.8	Weathered Basement(Saturated Clay)	
	175	-	-	Fractured Basement	
16	337	0.4	0.4	Top soil	H
	65	1.8	2.2	Weathered Basement (Clayey)	
	2590	-		Fresh basement	
17	272	2.9	2.9	Top soil	H
	13	4.9	7.9	Weathered Basement (Saturated clay)	
	121	-	-	Fractured Basement	
18	439	0.9	0.9	Top soil	H
	53	3.2	4.1	Weathered Basement (Clayey)	
	2576	-	-	Fresh Basement	
19	141	2.3	2.3	Top soil	H
	53	5.7	8.0	Weathered Basement (Clayey)	
	127	-	-	Fractured Basement	
20	319	0.5	0.5	Top soil	H
	127	1.5	2.0	Weathered basement (clayey sand)	
	303			Fractured Basement	
21	497	0.8	0.8	Top soil	H
	126	11.7	12.4	Sandy Clay	
	377	-	-	Weathered Basement	
22	182	1.0	1.0	Top soil	K
	248	8.0	9.0	Lateritic clay	
	161	-	-	Weathered basement (clayey sand)	

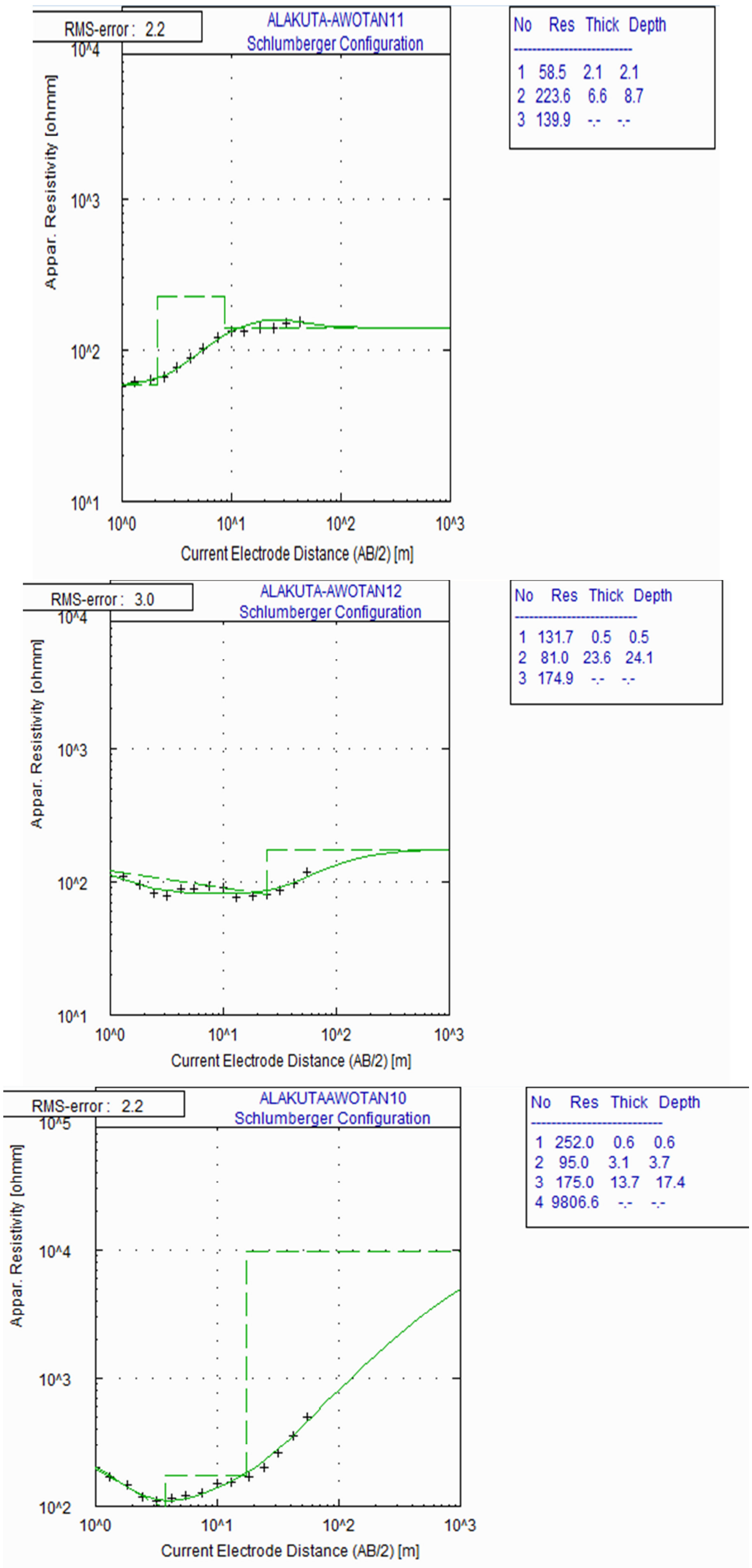

Fig 5 : Representative Layer model interpretation for ALAKUTA VES 11, 12 and 10.

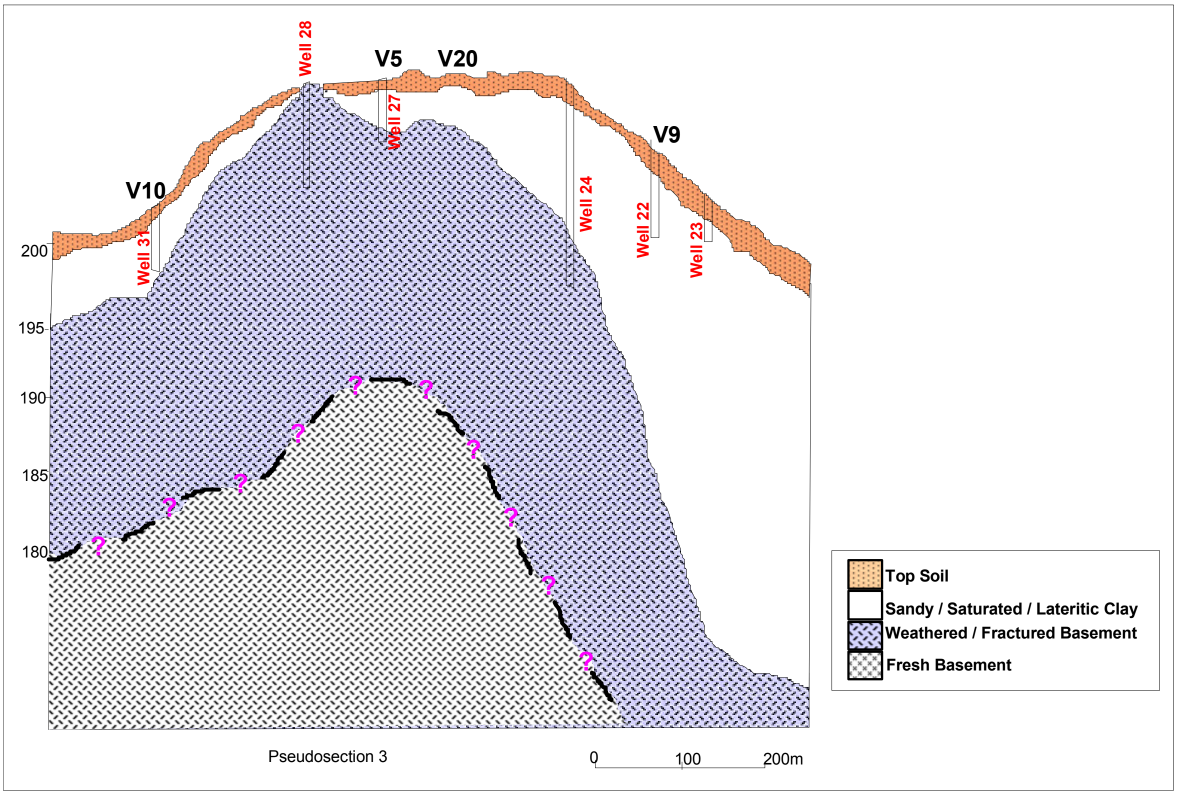

Figure 6a : Geoelectric section across V10, V5, V20 and V9

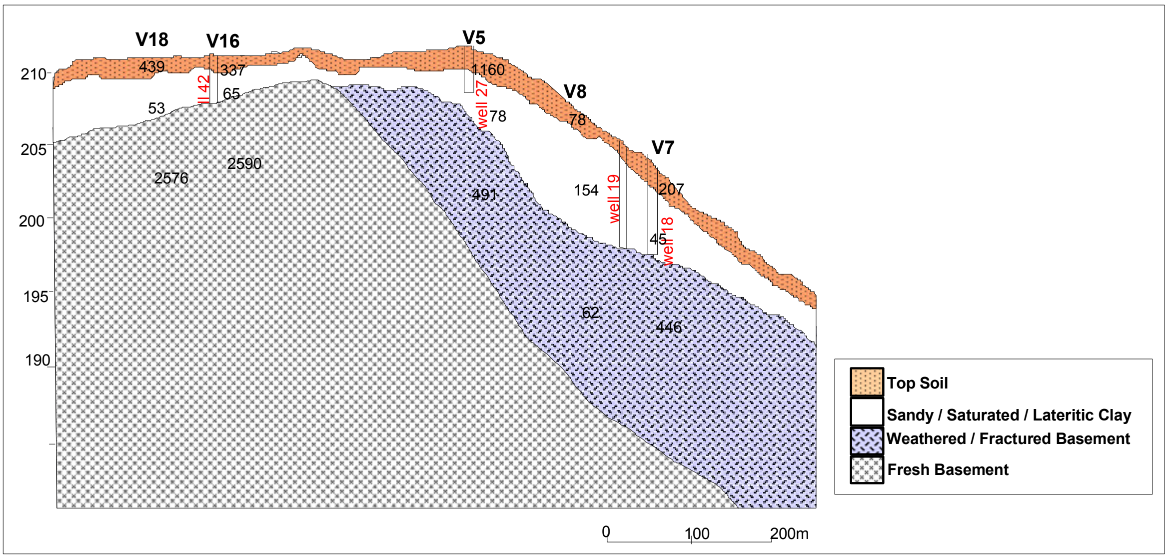

Figure 6b : Geoelectric section across V18, V16, V5, V8 and V7

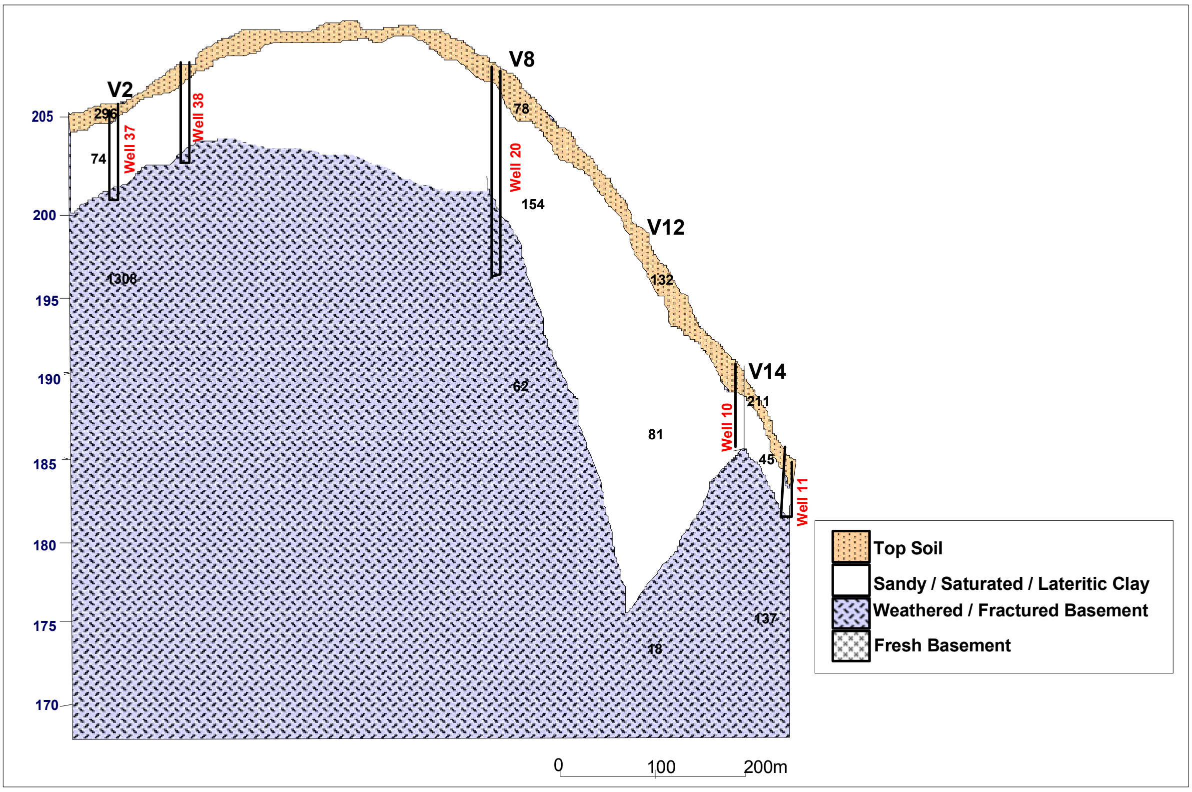

Figure 6C : Geoelectric section across V2, V8, V12 and V14

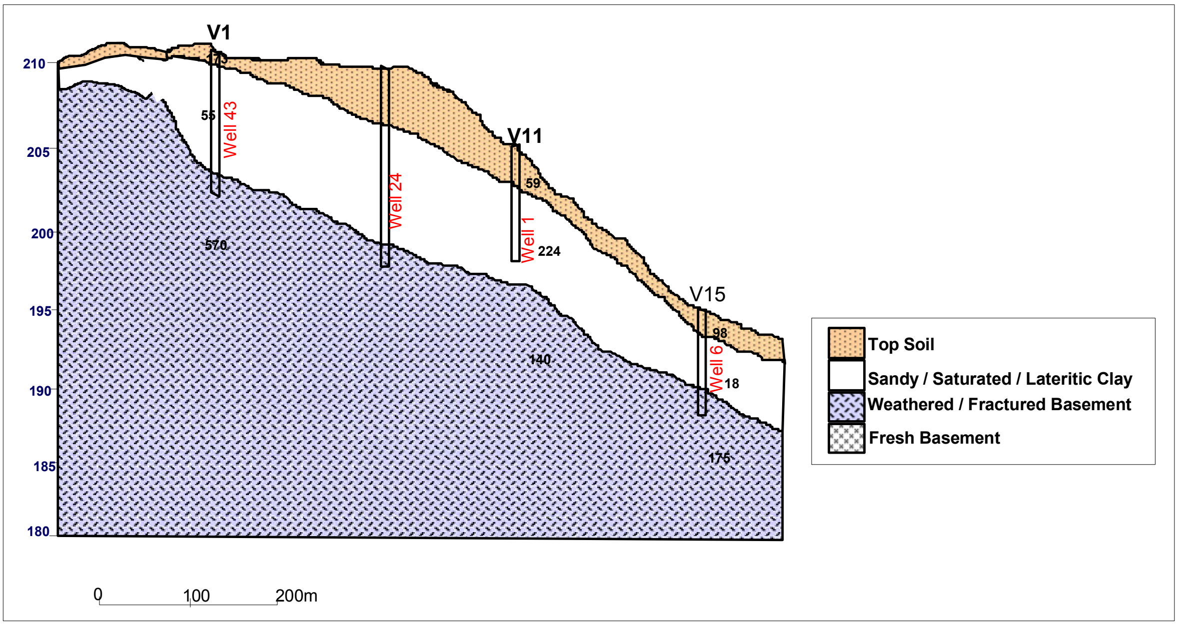

Figure 6D : Geoelectric section across V1, V11 and V15

Isopach map of the overburden

Figure 7 shows overburden thickness contoured map of the study area. The overburden thickness ranges from 0.4m to 24.1m with region of relatively high overburden thickness at the northern and southeastern part around V12, V7, V9, V13 whereas it is shallow towards the west around V2,V3,V5,V10, and V16.

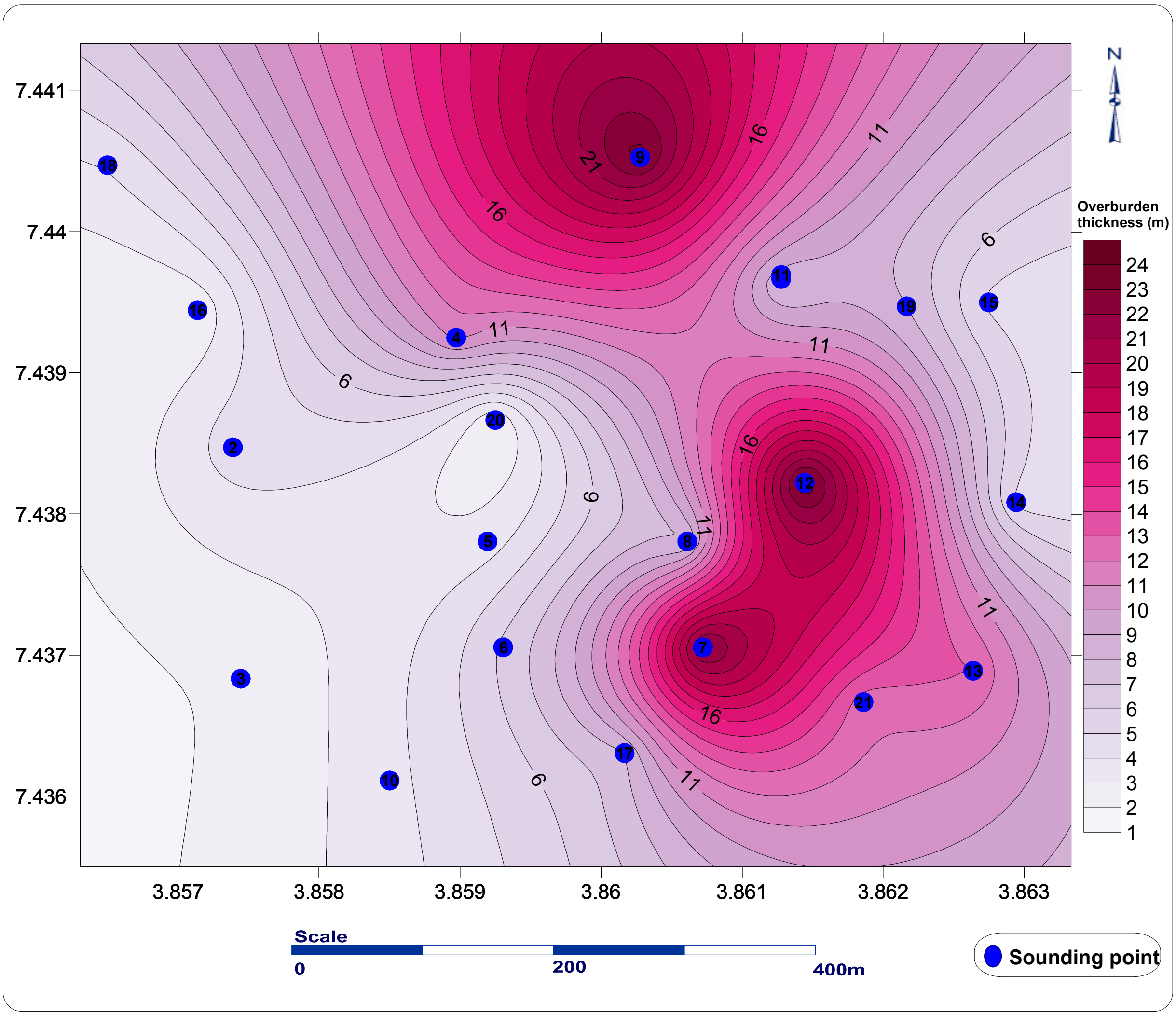

Figure 7. Isopach map of overburden

Radial Vertical Electrical Sounding

A consistent increase in the apparent anisotropy coefficient was observed for AB/2 spacing greater than 10 m and this behavior of increase in resistivity with depth may be due to the presence of the fracture effect at the corresponding true depths. Figure 8 a and b shows the polar plots for the variation of ρa data at four azimuths (0^0, 45^0, 90^0, 135^0) at various depths corresponding to the fractured basement at the six radial sounding locations. The observed changes in the apparent resistivity were interpreted as an indicator of fracture anisotropy. The fracture strikes at different depths are indicated as the polar plot trends. The survey identified three major fracture systems in the underlying basement rocks generally trending NE-SW, NW- SE and N-S of which NE-SW is the most prominent trend in Alakuta area. NE-SW trends are dominant at locations 1, 3 and 5 whereas NW- SE is prominent at locations 4 and 6 and N-S at location 2 (Fig 9). These trends are consistent with dominant orientation of structures on rock exposures within the study area and with the major fracture trend in Ibadan area as seen in the geological map (Fig 2). The plots of coefficient of apparent anisotropy against electrode spacing is also shown in figure 8a and b, this shows a general increase in the coefficient with depth.

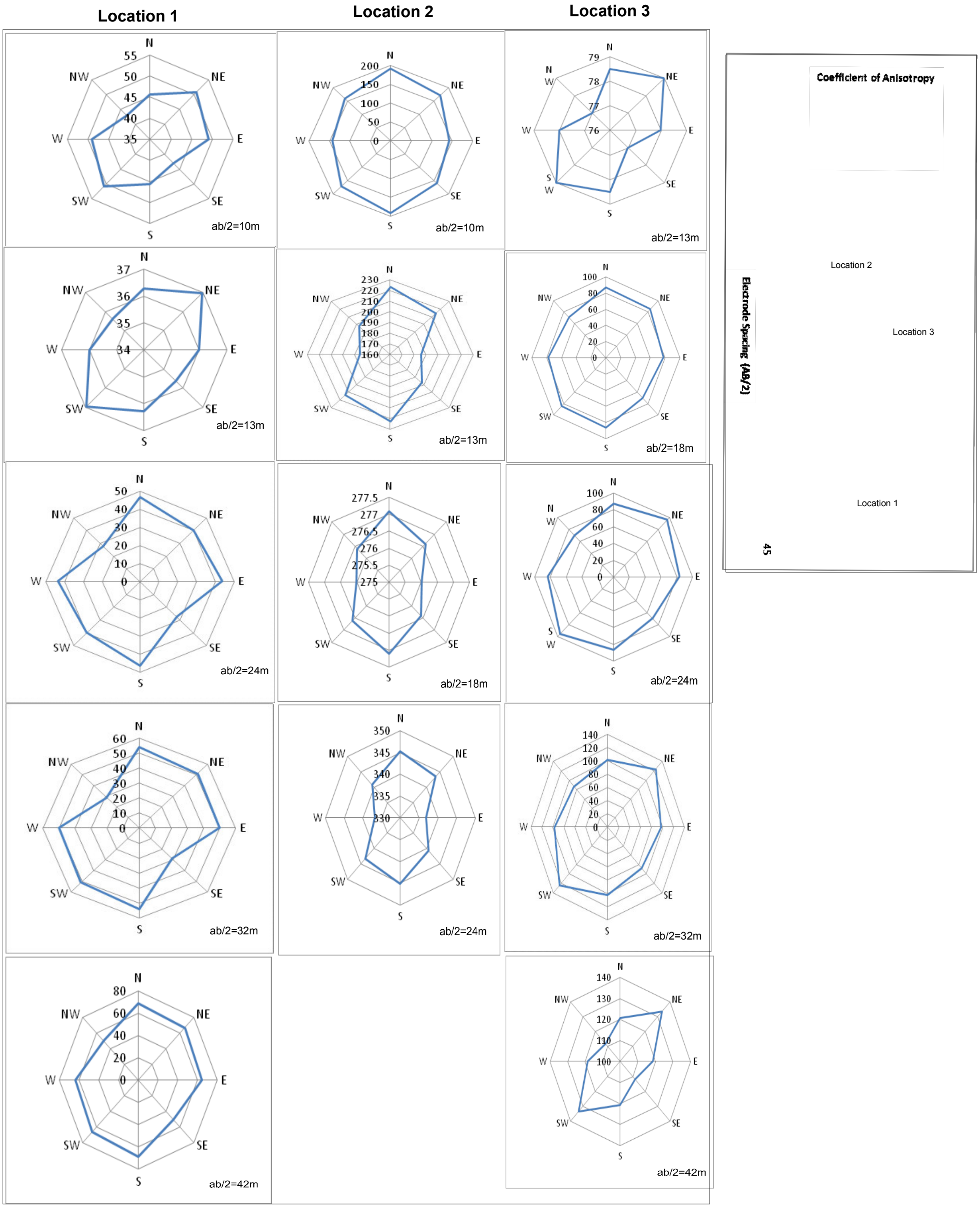

Figure 8a. Polar plots of apparent resistivity against azimuths at various depths corresponding to electrode spacing(a=10m-42m) and plot of apparent anisotropy against depth at locations 1,2 and 3.

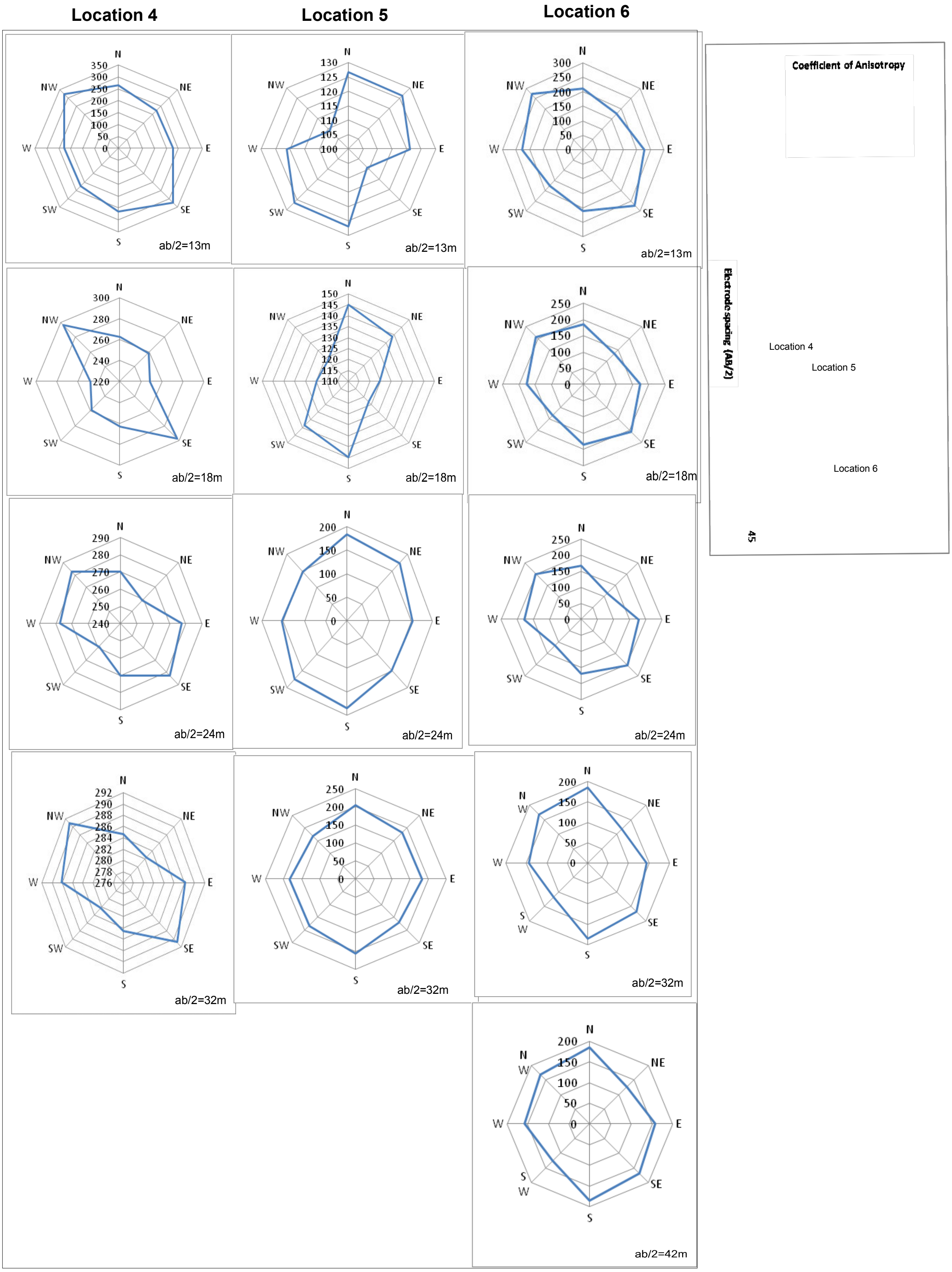

Figure 8b. Polar plots of apparent resistivity against azimuths at various depths corresponding to electrode spacing (a=10m-42m) and plot of apparent anisotropy against depth at locations 4, 5 and 6.

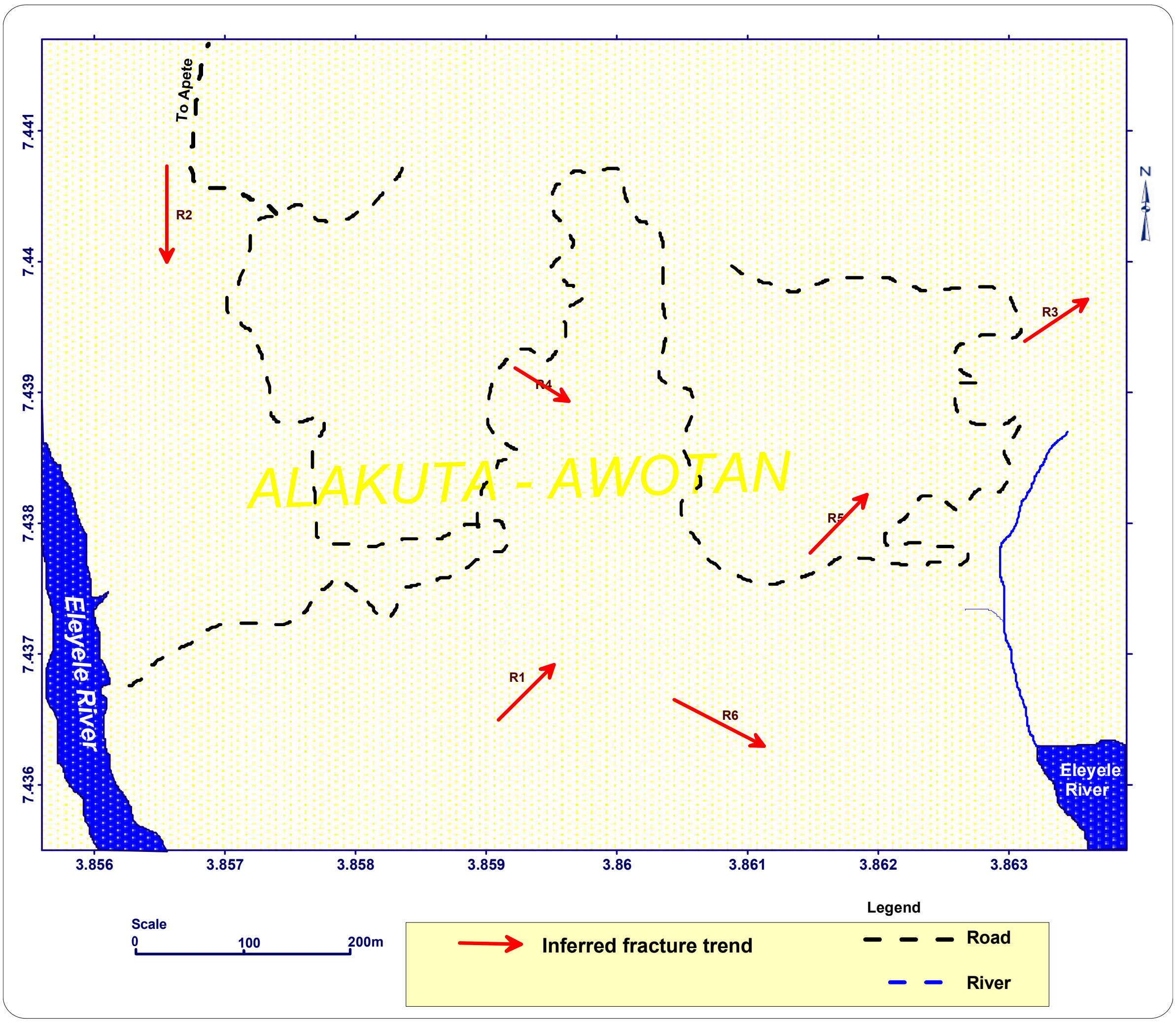

Figure 9. Map showing the inferred structural trends of fractures obtained from azimuth resistivity survey

At each measurement site, the resistivity data were used to estimate the characteristic fracture parameters, the fracture strike, the coefficient of anisotropy and the mean resistivity. These parameters are reported in Table 3.

Table 3. Characteristic fracture parameters at each subarea obtained from analysis of azimuthal resistivity data obtained from the study area.

Location	Electrode spacing (m)	Inferred fracture strike direction	Coefficient of Anisotropy, λ
1	13	NE-SW	1.03
	18	NE-SW	1.01
	24	NE-SW	1.21
	32	NE-SW	1.34
	42	NE-SW	1.15
2	13	N-S	1.16
	18	N-S	1.02
	24	N-S	1.06
3	18	NE-SW	1.1
	24	NE-SW	1.38
	32	NE-SW	1.19
	42	NE-SW	1.09
4	18	NW-SE	1.07
	24	NW-SE	1.05
5	13	NE-SW	1.07
	18	NE-SW	1.06
	24	NE-SW	1.12
	32	NE-SW	1.1
6	13	NE-SW	1.12
	18	NE-SW	1.24
	24	NE-SW	1.33
	32	NE-SW	1.2
	42	NE-SW	1.15

The coefficient of anisotropy (*λ)* has been shown to have the same functional form as permeability anisotropy to a first order (Bespalov et al., 2002). Thus, a higher coefficient of anisotropy (*λ)* implies higher-permeability anisotropy. The values of *λ* ranges from a minimum of 1.01 at Location 1 to a maximum of 1.38 at Location 3 (Table 2). The relatively higher values of *λ* at L1, L3 and L6 (1.34, 1.38 and 1.33) trending NE-SW suggests that the subsurface rocks in these areas are likely to be more intensely fractured and more permeable. In contrast, these indicative parameters at L2 (1.02 and 1.06) and L4 (1.07 and 1.05) suggest that the rock mass may be less intensely fractured and less permeable. These suggestions have obvious important implications in assessing groundwater transport and storage potential.

Discussion

Groundwater head (relief) map prepared from static water level shows that groundwater generally flow to the east and southwestern part of the study area. The water head ranges from 208m in the NW to 184m in the southeast above sea level. Two discharge sites and one recharge site R1were established in the flow map existing at the western and eastern part respectively. Also, the groundwater flow patterns show that river Eleyele and its tributaries probably recharged via the subsurface; therefore, this area is the discharge area.

Vertical Electrical Sounding also revealed three geologic units. These are: the top soil, the weathered layer and the partly weathered/fractured/fresh basement unit. The isopach map of the overburden show that the depth to the bedrock varies from 3m to 23m. This shows that the main aquifer (weathered basement) is relatively close to the surface. The main water – bearing unit in the area of study is the weathered basement and the fractured basement which are within the second and third geoelectric layers. The low resistivity (ranging from 62 to 863 Ohm – m) indicates presence of groundwater and the degree of weathering is very high. The weathered basement relief map delineates a series of ridges and depressions within the surveyed area. The depressions and the fractures zones (whose direction are delineated from the radial soundings) are the likely groundwater collecting centres and are priority areas for groundwater development.

The weathered/fractured basement is the main groundwater potential layer where the water is sourced in the study area and they have resistivity values that vary from 62 Ohm-m and 9807 Ohm-m with thickness values ranging from 2.2m to 36m (Table 1).

Conclusion

The hydro-geophysical investigation of ALAKUTA area has contributed to a better understanding of groundwater development in this part of the basement complex of southwestern Nigeria. Two aquiferous zones were delineated in the area. They are the weathered basement and fractured basement which occurred in almost all the locations. Basement depressions and/or fractured/sheared bedrock may likely contain more groundwater compared with areas where such structural features or elements are absent, since water often accumulates in the fractured/jointed column of the bedrock.

Radial vertical Electrical Sounding (VES) and surface geological studies show that significant joints and fractures occur along NE – SW, NW – SE and N-S directions. These studies further indicate relatively high coefficient of anisotropy of 1.33, 1.30 and 1.38 at the eastern and southern part of the study area, which shows relatively high permeability anisotropy at this region.

The technique has increased the rate of success for location of site for borehole drilling and consequently the cost effectiveness of groundwater exploration. Surface geophysical exploration of groundwater in Alakuta southwestern Nigerian therefore raises hope for water supplies in the area.

REFERENCES

Bespolov GD, Tabarovsky L, Schoen J (2002). on the relationship between resistivity and permeability anisotropy: Annual Technical Conference, Society of Petroleum Engineers, Proceedings, SPE 77715.

Busby, J. P. (2000). The effectiveness of Azimuthal apparent resistivity measurements as a method for determining fracture strike direction. Geophysical Prospecting, Vol. 148 pp 671-695

Busby, J. P. And Jackson, P. (2006), The application of time-lapse azimuthal apparent resistivity measurements for the prediction of coastal cliff failure, J. Appl. Geophy. 59, 261–272.

Cohn, M. E. And Rudman, A. J. (1995), Orientation of near-surface fractures from azimuthal measurements of apparent resistivity, SEG/Houston, Texas/95 Extended pp. 372–374.

Edet, A.E., Teme, S.C. Okereke, C.S. and Esu, E.O., (1994). Lineament Analysis for Groundwater Exploration in Precambrian Oban Massif and Obudu Plateau, S.E. Nigeria. *Jour. Of Min. Geol., 30(1). Pp. 87 – 95.*

Hagrey SA (1994). Electric study of fracture anisotropy at Falkenberg, Germany; Geophy., 59: 881-888.

Jones, H. A., and Hockey, R. D. (1964): The Geology of part of Southwestern, Nigeria. *Geol. Surv. of Nigeria Bull*., No. 31, 101p.

Lane, J. W., F. P. Haeni, and W. M. Watson, (1995). Use of a squarearray direct current resistivity method to detect fractures in crystalline bedrock in New Hampshire: Ground Water, 33, 476–485.

Leonard MPJ (1984). A Surface resistivity method for measuring hydrologic characteristics of jointed formations, U.S. Bur. Mines Report of Investigations 8901.

Mallik S. B., Bhattaccharya D. C.; Nag S. K. (1983). Behavior of Fractures in Hard Rocks- a Study by surface geology and radial VES method. Geoexploration, 21(3); 181-189.

Odoh I. B. and Onwuemes A. G., (2009). Estimation of anisotropic properties of fractures in Presco campus of Ebonyi State University AAbakaliki Nigeria using Azimuthal resistivity survey method.

Odusanya, B.O. and Amadi, U.M.P., (1990). An Empirical Resistivity Model for PredictingShallow Groundwater Occurrence in the (*Basement Complex Water Resources Journal of Nigeria Associat4ion of Hydrogeologist. 2, pp. 77 – 87.*

Olayinka, A. I. and Olorunfemi, M.O., (1992). Determination of Geoelectrical Characteristics in Okene Area and Implications for Borehole siting. *Journal of Mining and Geology, Vol. 28 (2), pp. 403 – 412.*

Olorunfemi, M.O. (1990). The hydrrogeological implication of topographic variation with overburden thickness in basement complex of southwestern Nigeria. *J. Min. Geol. Vol. 26, no. 1, pp. 145 – 152.*

Olorunfemi, M.O. and Ojo, J.S. and Akintunde, O.M., (1999). Hydrogeophysical Evaluation of the Groundwater Potential Akure Metropolis, Southwestern Nigeria. *Journal of Min. and Geology. Vol. 35 (2), pp. 207 – 228.*

Skjernaa L, Jorgensen N. O. (1993). Evaluation of Local Fracture Systems by Azimuthal Resistivity Surveys. Examples from south Norway. Int. J. Appli. Hydrogeol., 2: 19-25.

Taylor, R.W. and Flemming, A.H. (1988). Characterizing Jointed Systems by Azimuthal Resistivity Survey. Ground water, Vol. 26, pp 464-474

Watson, A.K. and Barkar, R.D. (1999). Differentiating Anisotropy and Lateral Effects Using Azimuthal Resistivity Offsets Wenner Sounding. Geophys. *Vol. 64, no. 3,pp. 739 – 745.*